2013

An improved SVD-based wall clutter mitigation method for through-the-wall radar imaging

Fok Hing Chi Tivive
University of Wollongong, tivive@uow.edu.au

Abdesselam Bouzerdoum
University of Wollongong, bouzer@uow.edu.au

Publication Details

F. Tivive & A. Bouzerdoum, "An improved SVD-based wall clutter mitigation method for through-the-wall radar imaging," in IEEE 14th Workshop on Signal Processing Advances in Wireless Communications (SPAWC), 2013, pp. 425-429.

An improved SVD-based wall clutter mitigation method for through-the-wall radar imaging

Abstract

This paper presents an improved SVD-based method for wall clutter mitigation in through-the-wall radar imaging. The dominant wall singular components are identified from the singular value spectrum. A subspace projection method is then applied to remove the strong wall clutter, residing in the dominant singular components, and separate the target signal from noise. The remaining wall clutter residual, which is mixed with the target signal, is suppressed by segmenting the range profile of the signal residing in the subspace orthogonal to the wall and noise subspaces. A Gaussian mixture is used to model the range profile, and the optimum segmentation threshold is found by minimizing the Bayes error. Experiments results show that the proposed method is more effective at reducing wall clutter and preserving the targets than some of the existing wall clutter mitigation methods.

Keywords

improved, clutter, wall, mitigation, imaging, radar, method, svd

Disciplines

Engineering | Science and Technology Studies

Publication Details

F. Tivive & A. Bouzerdoum, "An improved SVD-based wall clutter mitigation method for through-the-wall radar imaging," in IEEE 14th Workshop on Signal Processing Advances in Wireless Communications (SPAWC), 2013, pp. 425-429.

An Improved SVD-based Wall Clutter Mitigation Method for Through-the-Wall Radar Imaging

Fok Hing Chi Tivive and Abdesselam Bouzerdoum
School of Electrical, Computer and Telecommunications Engineering,
University of Wollongong,
Northfields Avenue, Wollongong NSW 2522, Australia
Email: {tivive, a.bouzerdoum}@uow.edu.au

***Abstract*—This paper presents an improved SVD-based method for wall clutter mitigation in through-the-wall radar imaging. The dominant wall singular components are identified from the singular value spectrum. A subspace projection method is then applied to remove the strong wall clutter, residing in the dominant singular components, and separate the target signal from noise. The remaining wall clutter residual, which is mixed with the target signal, is suppressed by segmenting the range profile of the signal residing in the subspace orthogonal to the wall and noise subspaces. A Gaussian mixture is used to model the range profile, and the optimum segmentation threshold is found by minimizing the Bayes error. Experiments results are presented which demonstrate that the proposed method is more effective at reducing wall clutter and preserving the targets than some of the existing wall clutter mitigation methods.**

***Keywords*—Wall clutter mitigation, Singular value decomposition, Gaussian mixture model, Stepped-frequency, Through-the-Wall Radar Imaging**

I. INTRODUCTION

Through-the-wall radar imaging (TWRI) has become a promising technology for sensing through obstacles and opaque materials, such as doors and walls, using wideband signals. TWRI can be used to detect stationary targets behind walls, and to determine the layout of the building. Recently, there has been an increasing interest in TWRI for surveillance in urban environments and search-and-rescue missions in natural disasters [1].

One of the main challenges in TWRI is the imaging of stationary targets behind the wall, which is usually a highly reflective and attenuative medium. Most of the TWRI studies dealing with stationary targets [2]–[4] assume prior knowledge of the background or reference scene, which is used in background subtraction prior to applying delay-and-sum beamforming. However, it is not always practical to obtain measurements from a reference scene devoid of targets. Several approaches, which do not rely on prior knowledge of the scene, have been proposed for wall clutter mitigation. In [5], multiple antenna arrays were used to suppress the wall returns in the received radar signals. Three antenna arrays are placed parallel to the wall at different heights, where the upper and lower arrays include receivers and the middle array consists of transmitters. Performing a simple subtraction of the radar returns from the lower and upper arrays can lead to wall clutter reduction. In this scheme, two additional arrays are required and the effect of the subtraction operation on the target reflections is unknown and cannot be controlled. In [6], a spatial filtering method was proposed for wall clutter mitigation. This method relies on invariance of the wall characteristics. This spatial invariance can be horizontal, vertical, or along both dimensions in the wall plane. A notch filter is applied across the array aperture to remove the zero-frequency or low spatial frequencies, which capture constant or slowly varying wall returns. Spatial filtering is effective when the wall is homogeneous and the array aperture is perfectly parallel to the wall surface; however, it may not work for walls with spatially varying characteristics or misaligned antenna arrays. Several SVD-based methods have been proposed for removing wall clutter from Bscan images [7]–[9]. The first eigen-image, associated with the most dominant singular value, was considered as the wall clutter, the second eigen-image was used for the target image, and the remaining eigen-components were considered as noise. Riaz and Ghafoor extended the SVD-based method by assuming the target returns span multiple eigen-components, while the wall clutter is represented by the first eigen-component [10]. More recently, we investigated the application of SVD to the raw radar signals, not the formed image, and showed that the wall and target subspaces can both be multi-dimensional [11], [12]. The dimension of the wall subspace depends on, among other factors, the wall electromagnetic characteristics and the alignment of the antenna array with respect to the surface of the wall. The dimension of the target subspace, on the other hand, is affected by the target location, the number of targets in the scene, and the antenna array configuration. The challenge of subspace methods is then to determine the dominant singular components that characterize the wall returns. Furthermore, due to the interactions between the wall and nearby targets, the remaining singular components, used to form the target image, may also contain wall clutter residual. In this paper, we propose a method to identify the dominant wall clutter components and to remove the wall clutter residual from the target signals. The proposed method does not rely on the estimation of the wall parameters nor does it require prior knowledge of the scene.

The remainder of the paper is organized as follows. The next section describes the geometric model of TWRI and presents briefly delay-and-sum beamforming. Section III describes the improved SVD-based wall clutter mitigation method. Experimental results are presented in Section IV. Finally, the conclusion is given in Section V.

II. THROUGH-THE-WALL SIGNAL MODEL

For high resolution TWRI, an N-element line array of transceivers is used to interrogate the scene behind the wall.

The line array can be either a physical array or a synthesized array aperture in which the transceiver is moved at different scan positions to form the full N-element array. In either case, the transceiver transmits a wideband signal with a desired range resolution. Figure 1 shows the geometric model of TWRI, where the wall plane is the (x, y) plane and the down-range is along the positive z axis. The n-th element of the array is placed at a certain standoff distance z_n, $n \in [0, N-1]$. In this paper, a ground-based stepped-frequency radar is used, where a wideband signal is synthesized by transmitting a series of monochromatic signals at M discrete frequencies, ω_m, $m \in [0, M-1]$, see [13] for a more detailed description.

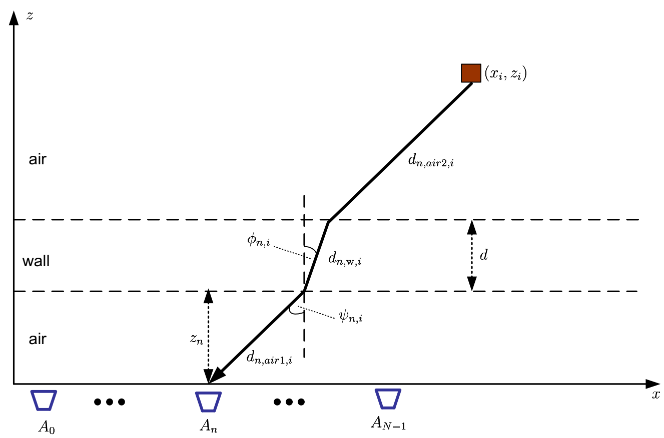

(a)

Fig. 1. Through-the-wall radar imaging geometry.

Here, we consider a homogeneous wall as a uniform dielectric slab. The reflection and transmission behavior of an electromagnetic plane wave incident on the wall can be found using Maxwell's equations. The reflection coefficient $\Gamma(k_m)$ of a lossless dielectric slab of thickness d is given by [15]

$$\Gamma(k_m) = \frac{\rho(1 - \exp(-j2\sqrt{\epsilon}k_m d))}{1 - \rho^2 \exp(-j2\sqrt{\epsilon}k_m d)}, \tag{1}$$

where ϵ is the relative permittivity of the wall, $k_m = \omega_m / c$ is the wave number corresponding to the m-th frequency, and ρ is the local Fresnel reflection coefficient given by

$$\rho = \frac{1 - \sqrt{\epsilon}}{1 + \sqrt{\epsilon}}. \tag{2}$$

The reflected radar signal at the m-th frequency received by the n-th antenna can be approximately written as

$$s_{\mathrm{w}}(m, n) = \frac{G\lambda_m}{8\pi} \frac{\exp(-j2k_m z_n)}{z_n} \Gamma(k_m), \tag{3}$$

where λ_m is the wavelength of the m-th transmitted monochromatic signal, G is the antenna gain and c is the speed of light in free space [16].

Suppose there are P targets in the scene. The transceiver transmits a perpendicularly polarized wave that is propagated at an oblique angle through the wall. The target signal of the m-th frequency received at the n-th antenna, due to the P targets, can be written as [14]:

$$s_{\mathrm{t}}(m, n) = \epsilon \frac{G\lambda_m}{4\pi} \sum_{i=1}^{P} C_{n,i} \sigma_i \exp(-j\omega_m \tau_{n,i}), \tag{4}$$

where ϵ is the relative permittivity of the wall, σ_i is the complex reflectivity of the i-th target, $\tau_{n,i}$ is the two-way propagation delay of the radar signal from the n-th antenna location to the i-th target at location (z_i, x_i). The parameter $C_{n,i}$ is given by

$$C_{n,i} = \frac{(T_{n,i})^4}{(d_{n,air1,i} + d_{n,\mathrm{w},i} + d_{n,air2,i})^2} \frac{\cos^2(\phi_{n,i})}{\cos^2(\psi_{n,i})}, \tag{5}$$

where $d_{n,air1,i}$, $d_{n,\mathrm{w},i}$, and $d_{n,air2,i}$ denote, respectively, the distances traveled by the signal from the n-th antenna to the i target at location (z_i, x_i) before, through, and after the wall, $\phi_{n,i}$ and $\psi_{n,i}$ are the incidence and refracted angles from the n-th antenna to the i-th pixel, respectively, and $T_{n,i}$ is the transmission coefficient from the i-th target received at the n-th antenna:

$$T_{n,i} = \frac{2\cos(\psi_{n,i})}{\cos(\psi_{n,i}) + \sqrt{\epsilon}\cos(\phi_{n,i})}. \tag{6}$$

By including the wall returns and target returns, the stepped-frequency signal of the m-th frequency received at the n-th antenna can be written as

$$s(m, n) = s_{\mathrm{w}}(m, n) + s_{\mathrm{t}}(m, n). \tag{7}$$

The scene can be represented with a rectangular grid of pixels. To form the image of the scene, delay-and-sum beamforming is applied to the radar signals collected across the array aperture. The complex amplitude of the q-th pixel of the image is computed as

$$I(q) = \frac{1}{NM} \sum_{n=0}^{N-1} \sum_{m=0}^{M-1} S(m, n) \exp\big(j\omega_m \tau_{n,q}\big), \tag{8}$$

where $\tau_{n,q}$ denotes the focusing delay applied to the n-th antenna output at the q-th pixel; for more details on the computation of the focussing delay in the presence of a wall, the reader is referred to [4].

III. Improved SVD-based Method

In our recent study [11], we have shown that when the elements of the array are misaligned, the wall reflections reside in a multidimensional subspace spanned by several dominant singular components. The challenge is to determine the dominant singular components for suppressing the wall returns and removing the wall clutter residual mixed with the target signal. The proposed SVD-based method for wall clutter mitigation consists of two stages. In the first stage, the strong wall reflections are suppressed through a subspace projection. . In the second stage, the wall clutter residual is separated from the target signal using a segmentation method applied to the range profile. Before the subspace projection, the radar signal is pre-processed to remove the common signal across the array aperture. Let S denote the $M \times N$ matrix of frequency-space measurements collected across the array aperture, $S = [s(m, n)], m = 0, ..., M-1, n = 0, ..., N-1$, where $s(m,n)$ is given by (7). After subtracting the common mean vector $\boldsymbol{m}$ from each column of S, we have the matrix

$$\widetilde{S} = S - \boldsymbol{m}\boldsymbol{e}^T, \tag{9}$$

where $\boldsymbol{e} = [1,\ldots,1]^T$ is an n-dimensional column vector. Using SVD, the matrix $\widetilde{S}$ can be expressed as

$$\widetilde{S} = \sum_{i=1}^{N} \lambda_i \boldsymbol{u}_i \boldsymbol{v}_i^H, \tag{10}$$

where H denotes the Hermitian transpose, $\boldsymbol{u}_i$ and $\boldsymbol{v}_i$ are the i-th left and right singular vectors, respectively, and λ_i is the i-th singular value, arranged in descending order of their magnitudes.

Since the wall reflections are relatively stronger than the target reflections, it is assumed that the strong wall reflections are characterized by the first few dominant singular components. To determine the number of dominant singular components spanning the wall subspace, we develop a technique to identify their corresponding singular values from the singular value spectrum. Suppose the range of singular values is $[0,\lambda_1]$, where λ_1 is the largest singular value. We can use a threshold $\gamma \in [0,\lambda_1]$ that will partition the singular value spectrum into two classes: $\mathcal{C}_\mathrm{w} = \{\lambda_i \geq \gamma\}$ and $\mathcal{C}_\mathrm{t} = \{\lambda_i < \gamma\}$. Here, we employ Otsu's method [18], which computes the optimum threshold by maximizing the between-class variance:

$$\sigma_b^2(k) = \pi_\mathrm{w}(k)\pi_\mathrm{t}(k)[\mu_\mathrm{w}(k) - \mu_\mathrm{t}(k)]^2, \tag{11}$$

where $\pi_\mathrm{w}(k)$ and $\pi_\mathrm{t}(k)$ are the class probabilities separated by a threshold k and μ_w and μ_t are the class means. Using the singular vectors of the wall class, we can form the projection matrix of the wall subspace as

$$\mathbf{P}_\mathrm{w} = \sum_{i\in\mathcal{W}} \boldsymbol{u}_i \boldsymbol{v}_i^H, \tag{12}$$

where $\mathcal{W}$ is the set of indices of wall singular values. The projection matrix onto the subspace orthogonal to the wall subspace is computed as

$$\mathbf{P}_\mathrm{w}^\perp = \mathbf{I} - \mathbf{P}_\mathrm{w}\mathbf{P}_\mathrm{w}^H, \tag{13}$$

where $\mathbf{I}$ denotes the identity matrix. To suppress the strong wall reflections, the matrix $\widetilde{S}$ is projected onto the orthogonal subspace:

$$\widehat{S} = \mathbf{P}_\mathrm{w}^\perp \widetilde{S}. \tag{14}$$

The remaining signals in the matrix $\widehat{S}$ comprise the target signal, noise, and some wall clutter residual. To remove the noise, the radar signals are further projected onto the subspace orthogonal to the noise subspace,

$$\bar{B} = (\mathbf{I} - \mathbf{P}_\mathrm{n}\mathbf{P}_\mathrm{n}^H)\widehat{B}, \tag{15}$$

where $\mathbf{P}_\mathrm{n} = \sum_{i\in\mathcal{N}} \boldsymbol{u}_i \boldsymbol{v}_i^H$ is the noise subspace and $\mathcal{N}$ is the index set of the noise singular values. To identify the noise subspace, Akaike Information Criterion (AIC) or Minimum Description Length (MDL) methods can be used to determine noise singular values.

After the subspace projection, the radar signals may still contain wall clutter residual, due to the interactions between the wall and nearby targets. Here, we propose a segmentation method to remove the wall clutter residual from the range profile of the radar signal. Let $\bar{\boldsymbol{b}}_n = [b_0,\ldots,b_{M-1}]$ denote the n-th column of $\bar{B}$. The range profile of the n-th antenna can be computed as

$$R_n(r) = \frac{1}{M}\sum_{k=0}^{M-1} b_k \exp(j2\pi rk/M), \tag{16}$$

The overall range profile of the radar signals is then expressed as

$$A(r) = \sum_{n=0}^{N-1} |R_n(r)|, \tag{17}$$

After normalizing $A(r)$, we can model the overall range profile as a mixture of Gaussian distributions. We use the Gaussian mixture (GM) to model the overall range profile. Then, then Gaussian components of the mixture are classified into wall and target components, and an optimum range is determined to segregate the target signal and the wall clutter residual. Using the Expectation Maximization algorithm to estimate the parameters of the GM, we model the overall range profile as

$$p(r) = \sum_{k=1}^{K} w_k g(r|\mu_k,\sigma_k^2) \tag{18}$$

where w_k is the mixture weight, μ_k is the mean, and σ_k^2 is the variance of the k-th gaussian component, K is the number of Gaussian components, $g(r)$ is the gaussian component given by

$$g(r) = \frac{1}{\sqrt{2\pi\sigma^2}}\exp\{-\frac{(r-\mu)^2}{2\sigma^2}\}. \tag{19}$$

The optimum number of mixture components K is determined by minimizing the Bayesian information criterion.

In order to segment the wall residual from the target signal, we first identify the Gaussian components associated with the wall clutter residual. This can be done by estimating the wall range from the dominant wall singular components spanning the wall subspace found in the first stage. Let ρ_i denote the range associated with the main peak of the range profile obtained from the i-th dominant singular component. The wall range can be estimated as

$$r_\mathrm{w} = \max_{i\in\mathcal{W}}(\rho_i). \tag{20}$$

Now, we can classify the Gaussian components into wall and target classes. The Gaussian components whose mean values are within the wall range, r_w, are labeled as wall components and their indices are stored in the index set $\mathcal{I}_\mathrm{w}$. The remaining Gaussian components are considered as target components; their indices are stored in the index set $\mathcal{I}_\mathrm{t}$. The probability density functions of the wall residual and target can be expressed as

$$p_\mathrm{w}(r) = \frac{1}{\sum_{i\in\mathcal{I}_\mathrm{w}} w_i}\sum_{i\in\mathcal{I}_\mathrm{w}} w_i g(r|\mu_i,\sigma_i^2) \tag{21}$$

and

$$p_\mathrm{t}(r) = \frac{1}{\sum_{i\in\mathcal{I}_\mathrm{t}} w_i}\sum_{i\in\mathcal{I}_\mathrm{t}} w_i g(r|\mu_i,\sigma_i^2). \tag{22}$$

The optimum segmentation threshold η that segregates the wall residual and the target is computed by minimizing the Bayes error given by

$$E(\eta) = \int_{-\infty}^{\eta} p_{\mathrm{t}}(r)\mathrm{d}r + \int_{\eta}^{\infty} p_{\mathrm{w}}(r)\mathrm{d}r, \qquad (23)$$

By differentiating the objective function given in (23) and setting the derivative to zero, the optimum segmentation threshold can be obtained. Thus, using the Leibnitz differentiation rule, we get

$$\frac{\mathrm{d}E(\eta)}{\mathrm{d}\eta} = p_{\mathrm{t}}(\eta) - p_{\mathrm{w}}(\eta) = 0, \qquad (24)$$

A root-finding algorithm such as Newton-Raphson or Secant method is then used to find the optimum threshold η. Using the optimum threshold η, we segment the range profile associated with the radar signal received at the n-th antenna as

$$\widehat{R}_n(r) = \begin{cases} R_n(r) & \text{if } r > \eta \\ 0 & \text{otherwise} \end{cases}, \quad n \in [0, N-1]. \qquad (25)$$

Discrete Fourier transform is then used to convert the range profiles into the frequency-space measurements before applying DS beamforming. In the next section, the proposed SVD-based method is tested on simulated data and compared with other wall clutter mitigation methods.

IV. Experimental Results

To evaluate the proposed SVD-based method for wall clutter mitigation, we simulate a TWRI scene with two targets behind a lossless homogeneous wall. The homogeneous wall has a thickness of 0.2 m and a dielectric constant of 6.5. Two targets are placed behind the wall at the coordinates $(-1,\ 0.8)$ m and $(1,\ 2)$ m. A 71-element array is placed at a standoff distance of 1 m from the wall and is tilted at an angle of 0.3 degree with respect to the front surface of the wall. The transmitted stepped-frequency signal has a bandwidth of 2 GHz centered at 2 GHz with a step size of 5 MHz. Several wall clutter mitigation methods, namely background subtraction, time-gating, spatial filtering, and the wall clutter mitigation methods described in [9], [10], are implemented, and their performance are compared with that of the proposed method. The wall clutter mitigation method is assessed in terms of the improvement factor (IF) of the target-to-clutter ratio (TCR). The IF of a formed image is computed as

$$\mathrm{IF} = 10\log\left(\frac{\mathrm{TCR}_1}{\mathrm{TCR}_0}\right), \qquad (26)$$

where TCR_0 and TCR_1 are, respectively, the target-to-clutter ratios of the formed image before and after wall clutter mitigation. The TCR of a formed image is computed as

$$\mathrm{TCR}_\nu = \frac{\frac{1}{N_t}\sum_{q\in A_t}|I_\nu(q)|}{\frac{1}{N_c}\sum_{q\in A_c}|I_\nu(q)|}, \quad \nu = 0, 1 \qquad (27)$$

where A_{t} is the target region, N_{t} is the number of pixels in the target region, A_{c} is the clutter region, N_{c} is the number of clutter pixels, and $I_0(q)$ and $I_1(q)$ are formed images before and after wall clutter mitigation, respectively.

Figure 2(a) shows a cluttered image when applying DS beamforming directly to the frequency-space measurements without wall clutter mitigation. After the subspace projection in the first stage, the proposed method significantly suppresses the wall clutter, as shown in Fig. 2(b), but the image still has some wall clutter residual. Figure 3 shows the beamformed images produced by the different wall clutter mitigation methods. Figure 3(a) shows removing the first three dominant singular components suppresses the wall clutter as well as distorts the target near the wall. Figures 3(b)–(d) illustrate the output images after time gating, spatial filtering, and the image-based SVD method with AIC, respectively. In these images, the wall clutter is still too strong for the targets to be visible. One possible reason why time gating can not remove the wall returns is that the wall reverberations and the target reflections overlap in the time domain. For spatial filtering, it can mitigate the wall returns when the array aperture is parallel to the wall. However, in our simulation, there is a misalignment of the line array with respect to the surface of the wall. The Bscan-based and image-based SVD methods [9], [10] cannot suppress the wall clutter as they assume that the wall clutter spans only the first eigen-image. On the other hand, the proposed SVD-based method produces an image, depicted in Fig. 3(e), which is as clear as that of background subtraction, cf. Fig. 3(f).

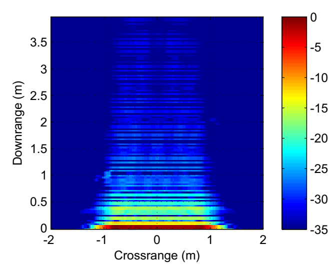

(a)

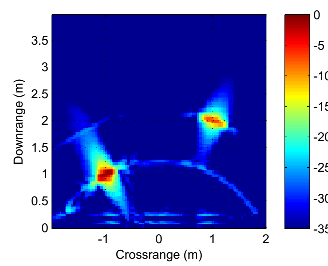

(b)

Fig. 2. Formed image before and after using the proposed method: (a) no wall clutter mitigation and (b) after the first stage of the proposed method. The formed images are displayed in log scale in dB.

Table I lists the performances of the wall clutter mitigation methods in terms of IF and TCR. In the table, we also present the IF and TCR of the image after manually removing the first few dominant singular components. By discarding the most dominant singular component, we obtain an image with IF = 2.36 dB and TCR = 4.31 dB. Removing the first two dominant singular components gives an IF of 12.01 dB and TCR of 13.91 dB. Discarding other leading singular components deteriorates the IF and TCR of the formed image. For example, removing the first three leading singular components decreases the IF to 10.96 dB and the TCR to 10.93 dB. The proposed method gives the best IF and TCR, except for background subtraction.

TABLE I. Target-to-clutter ratio and improvement factor of the wall clutter mitigation methods.

Approach	TCR_1 (dB)	IF (dB)
Background subtraction	15.84	12.58
Proposed wall mitigation method	15.82	12.57
Removing first dominant singular component	2.36	4.31
Removing first two dominant singular components	13.91	12.01
Removing first three dominant singular components	10.93	10.96
Removing first four dominant singular components	10.21	10.67
Bscan-based SVD method described in [9]	1.29	1.18
Image-based SVD method described in [10]	1.30	1.70
Spatial filtering	2.23	4.05
Time gating	1.59	2.60

V. Conclusion

In this paper, an improved SVD-based method was proposed for wall clutter mitigation in TWRI. The proposed wall clutter mitigation method firstly determines the dominant singular components that lie in the wall subspace. Then, it projects the radar signal onto the subspace orthogonal to the wall subspace to remove the strong wall returns. A subspace projection is also applied to separate the target signal from noise. Finally, a segmentation technique is applied to the range profile to remove the residual wall clutter interacting with the target signal. Experiments results showed that the proposed method achieves better results than other existing wall clutter mitigation methods.

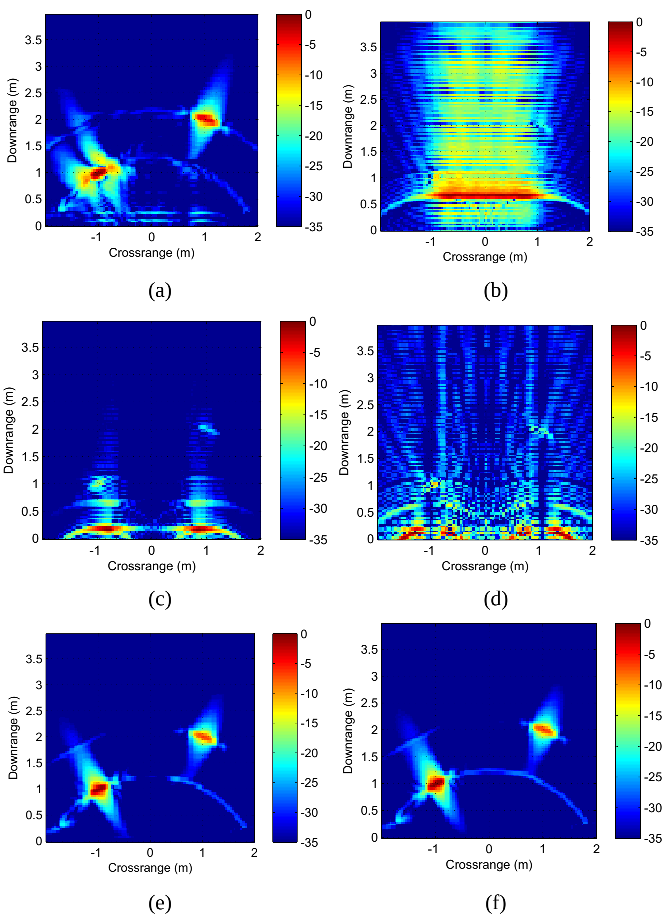

Fig. 3. Images obtained from different wall clutter mitigation techniques: (a) after removing of the first three singular components, (b) time gating, (c) spatial filtering, (d) image-based SVD method with AIC, (e) proposed SVD-based method, and (f) background subtraction. The formed images are displayed in log scale in dB.

Acknowledgement

This work is supported by a grant from the Australian Research Council (ARC).

References

[1] M. G. Amin, Ed., *Through-the-wall radar imaging*, CRC Press, Boca Raton, FL, 2011.

[2] R. Dilsavor, W. Ailes, P. Rush, F. Ahmad, W. Keichel, G. Titi, and M. Amin, "Experiments on wideband through the wall imaging," in *Proc. SPIE Symposium on Defense and Security, Algorithms for Synthetic Aperture Radar Imagery XII Conf.*, vol. 5808, 2005, pp. 196–209.

[3] J. Moulton, S. A. Kassam, F. Ahmad, M. G. Amin, and K. Yemelyanov, "Target and change detection in synthetic aperture radar sensing of urban structures," in *Proc. IEEE Radar Conference*, 2008, pp. 1–6.

[4] F. Ahmad, Y. Zhang, and M. G. Amin, "Three-dimensional wideband beamforming for imaging through a single wall," *IEEE Geoscience and Remote Sensing Letters*, vol. 5, no. 2, pp. 176–179, 2008.

[5] M. Dehmollaian and K. Sarabandi, "Analytical, numerical, and experimental methods for through-the-wall radar imaging," in *IEEE International Conference on Acoustics, Speech and Signal Processing*, 2008, pp. 5181–5184.

[6] Y.-S. Yoon and M. G. Amin, "Spatial filtering for wall-clutter mitigation in through-the-wall radar imaging," *IEEE Transactions on Geoscience and Remote Sensing*, vol. 47, no. 9, pp. 3192–3208, 2009.

[7] A. N. Gaikwad, D. Singh, and M. J. Nigam, "Study of effect of room window on through wall imaging in uwb range," in *International Conference on Emerging Trends in Electronic and Photonic Devices and Systems*, 2009, pp. 395–398.

[8] R. Chandra, A. N. Gaikwad, D. Singh, and M. J. Nigam, "An approach to remove the clutter and detect the target for ultra-wideband through-wall imaging," *Journal of Geophysics and Engineering*, vol. 5, no. 4, pp. 412–419, 2008.

[9] P. K. Verma, A. N. Gaikwad, D. Singh, and M. J. Nigam, "Analysis of clutter reduction techniques for through wall imaging in UWB range," *Progress in Electromagnetics Research B*, vol. 17, pp. 29–48, 2009.

[10] M. M. Riaz and A. Ghafoor, "Through-wall image enhancement based on singular value decomposition," *International Journal of Antennas and Propagation*, vol. 2012, no. Article ID 961829, p. 20 pages, 2012.

[11] F. H. C. Tivive, M. G. Amin, and A. Bouzerdoum, "Wall clutter mitigation based on eigen-analysis in through-the-wall radar imaging," in *Proc. of International Conference on Digital Signal Processing*, 2011, pp. 1–8.

[12] F. H. C. Tivive, A. Bouzerdoum, and Moeness G. Amin, "An SVD-based approach for mitigating wall reflections in through-the-wall radar imaging," in *Proc. IEEE Radar Conference*, 2011, pp. 519–524.

[13] F. Ahmad, M. G. Amin, and S. A. Kassam, "Synthetic aperture beamformer for imaging through a dielectric wall," *IEEE Transactions on Aerospace and Electronic Systems*, no. 1, pp. 271–283, 2005.

[14] R. Linnehan, J. Schindler, D. Brady, R. Kozma, R. Deming, and L. Perlovsky, "Dynamic logic applied to SAR data for parameter estimation behind walls," in *Proc. IEEE Radar Conference*, 2007, pp. 850–885.

[15] C. A. Balanis, *Advanced Engineering Electromagnetics*, NY: John Wiley and Sons, 1989.

[16] M. Dehmollaian and K. Sarabandi, "Refocusing through building walls using synthetic aperture radar," *IEEE Transactions on GeoScience and Remote Sensing*, vol. 46, no. 6, pp. 1589–1599, 2008.

[17] Y.-S. Yoon and M. G. Amin, "High-resolution through-the-wall radar imaging using beamspace music," *IEEE Transactions on Antennas and Propagation*, vol. 56, no. 6, pp. 1763–1774, 2008.

[18] N. Otsu, "A threshold selection method for gray level histograms," *IEEE Transactions on Systems, Man, and Cybernetics*, vol. 9, no. 1, pp. 62–66, 1979.